Scientia Iranica (2024) 31(9), 681–691

Sharif University of Technology
Scientia Iranica
Transactions C: Chemistry and Chemical Engineering
https://scientiairanica.sharif.edu

Exfoliated poly (styrene-*co*-urethane) grafted-poly methylmethacrylate/layered double hydroxide nanocomposite synthesized by metal catalyzed living radical polymerization and solvent blending method

M. Hosseinzadeh[a,*], S. Ghasemi Karaj-Abad[b,*], M. Rasizadeh[b], and M. Abbasian[c]

a. *Marand Faculty of Technical and Engineering, University of Tabriz 5166616471, Tabriz, Iran.*
b. *Department of Chemistry, Payame Noor University, P.O. Box. 19395-3697, Tehran, Iran.*
c. *Department of Polymer, Engineering Faculty, University of Bonab, Bonab 55517, Iran.*

Received 10 February 2022; received in revised form 16 July 2023; accepted 3 September 2023

KEYWORDS
Graft copolymer;
Poly (styrene-*co*-urethane);
ATRP;
LDH;
Nanoparticles.

Abstract. In this research, a facile strategy was employed for the synthesis of terpolymer derivatives from polystyrene (PSt), polyurethane (PU), poly (methyl methacrylate) (PMMA), and its organo-modified Zn Al LDH (layered double hydroxide) by *in situ* Atom Transfer Radical Polymerization (ATRP). For this purpose, firstly, LDH nanoparticles were modified with Sodium Dodecyl Sulfonate (SDS) by the anion exchange reaction of Zn-Al-LDH. Secondly, PU macroinitiator was obtained from a solvent composed of 9-decen-1-ol and used in controlled graft copolymerization of styrene monomer to afford PU-*co*-Pst copolymer. Then, the synthesized PU-*co*-St was brominated by N-bromosuccinimide (NBS) to obtain a copolymer with the bromine group. In the following, living radical polymerization of Methyl Methacrylate (MMA) was done in the presence of brominated PU-*co*-St and CuBr/Bpy (2,2′-bipyridine catalyst to prepare the (PMMA-*g*-PSt-*g*-PU) terpolymer. Finally, (PMMA-*g*-PSt-*g*-PU)/ZnAl LDH nanocomposite was successfully synthesized by the solution intercalation method. FE-SEM images showed that surface morphologies of Zn-Al (SDS) and Zn-Al-LDH leads to sheet-like and hexagonal morphology. Investigation of thermal properties using DSC and TGA exhibited that the (PMMA-*g*-PSt-*g*-PU)/Zn-Al-LDH nanocomposite has a higher thermal stability compared to neat PU. The synthesized terpolymer and (PMMA-*g*-PSt-*g*-PU)/Zn-Al-LDH nanocomposite can be used as a reinforcing agent for polymeric nanocomposites due to its high LDH properties.

1. Introduction

Due to their low cost and excellent physical properties, polyolefin-based polymers have recently acquired vast applications in various fields of economy, technology and daily life. This type of versatile polymers makes the most important section of the shopper market, relatively since they are generally used in domestic

*. *Corresponding author. E-mail address: m.hosseinzadeh@tabrizu.ac.ir (M. Hosseinzadeh);*

To cite this article:
M. Hosseinzadeh, S. Ghasemi Karaj-Abad, M. Rasizadeh, and M. Abbasian "Exfoliated poly (styrene-*co*-urethane) grafted-polymethylmethacrylate/layered double hydroxide nanocomposite synthesized by metal catalyzed living radical polymerization and solvent blending method", *Scientia Iranica* (2024), **31**(9), pp. 681-691. DOI: 10.24200/sci.2023.59942.6507

products and good industrial polymeric material [1–3]. The polymers resins based of polyolefin, for example, polyethylene (PE), polypropylene (PP), polystyrene (PSt), and polyvinyl chloride (PVC), have been often utilized. Their mechanical strength, excellent performance, and feasibility create them fully practicable and variable; however, one of the most important drawbacks of these polymeric materials, is low impact resistance. Therefore, researchers are trying to modify this property [4].

On the other hand, polyurethane (PU) has unique affect resistance, hydrolytic, thermal stability, excellent mechanical strength, chemical and physical resistance. Polyurethane has been used in automobiles, coating, variable foams for floors, composites, and stiff foams used as an insulating polymeric material of refrigerators, reaction molding fibers, plastics, paints, sticky, buildings, and thermoplastic elastomer [5–7].

Polyurethane is the most abundant types of organic polymers that have attracted most attention after PE, PP, PSt, and PVC in market. It is the most abundant utilized in thermosetting resins. Also, it has unique properties such as flexibility and elasticity compared to rubber. Low in vitro protein adsorption of polyurethane is relatively permanent in contact with body fluids, e.g., blood and plasma. To modify heat resistance, blending and grafting of polyurethane with polymers based of polyolefin is very important [8]. The composites in blend form were presented to be used to modify for drawbacks of the monopolized polymers [9]. However, drawbacks occur in the blending of hydrophobic polymers based on polyolefin and in hydrophilic polyurethane polymer. This blending can be performed using surfactants, chemical additives, and polymer modification methods [10].

The graft polymerization method is a polymerization technique employed for branching a polyolefin-based polymer onto a layered polymer with a wide-range of monomers. The obtained polymers by grafting methods are resistant and protect their natural features [11,12]. The natural polymer modification methods utilize radical polymerization, chemical modification, radiation, and plasma [13].

It has been confirmed that the physicochemical properties of polymers with the well-defined structures are completely related to their molecular signs, for example, molecular weight distribution (low polydispersity, Mw/MO), Degree of Polymerization (DP), molecular weight as well as number, type and spatial situations of effective groups in the copolymer backbone [14–16]. Furthermore, the physicochemical properties of the graft copolymers are completely different from blends of the same corresponding homopolymers [17,18]. From this conceptual point of view, Reversible Deactivation Radical Polymerization (RDRP), which is communally known as 'living' or controlled radical polymerization, approaches including NMP (Nitroxide-Mediated Polymerization), RAFT (Reversible Addition of Fragmentation chain Transfer), and ATRP (Atom Transfer Radical Polymerization), have been extended as important and essential approaches for the synthesizing of graft copolymers with complex macromolecular architectures, narrow dispersity and controlled molecular weight [19–30].

Among these, ATRP is an efficient and promising strategy due to its accurately controlling of the molecular weight, low dispersity and well-defined macromolecular architecture, as well as variety of a great chain end-functionalities. Other superiorities of the ATRP method are making of negligible homopolymer when applied in graft copolymers, simple experimental condition and also applicable to a wide range of monomers possessing with different polarities and functional groups. Furthermore, it has unique endurance to many additives, solvents and impurities [31,32].

ATRP by means conversion metal (likewise nickel, ruthenium, copper, etc) dormant alkyl halides complexes with (2,2′-bipyridine) derivative for graft polymerization of numerous monomers, such as acrylates, styrene, methacrylate's, etc [19,20].

Accordingly, to maintain a low condensation of active species, ATRP employ the equilibrium between active propagating radicals and dormant alkyl halide complexes. The activated radical species can be deactivated to remake the dormant species or propagate [33].

In the past few years, nanotechnology has presented an excellent novel facility for the development of novel affective polymeric substances with modified physicochemical properties in various fields, such as chemistry, engineering, biology and so on.

PCNs (Polymer/Clay Nanocomposites) have received more attention in the field of nanotechnology [17,34,35]. It is proved that the mechanical properties of polymer (e.g., thermal stability, permeability, dimensional, increased stiffness strength, gas barrier, flame retardancy) are extraordinary modified and new excellent properties may be revealed after the increase of only a little content of clay to the polymer matrix (about 5 w.t%) [36–39].

PCNs can be synthesized using three main approaches including melt intercalation, in situ polymerization and solution exfoliation/intercalation [39,40].

Furthermore, the stability of interfacial interactions between the clay layers and polymer matrix, creates three different structures thermodynamically [34,39]. A conventional micro composite is formed and d_{001} of clay remnants unchanged when the polymer chain does not permeate the silicate layers. The polymer chains tend to penetrate between the platelets that leads to an increase in d_{001} if there is some grafting between the polymer and the clay. In this case, the silicates layers remain bulked and the resulting com-

posite is an intercalated microstructure. Accordingly, an exfoliated morphology can be prepared when the interaction is proper between the silicate and polymer and the silicate layers are entirely pushed apart to develop a disordered row [34,39,41].

The objective of this research, represents the development of a novel and effective strategy for synthesizing (PMMA-*g*-PSt-*g*-PU)/ZnAl LDH nanocomposite *via* a combination of ATRP polymerization and solution intercalation methods. Using this new method, we can control the molecular weight of grafting onto polyurethane. On the basis of our science, no research work has been studied on the research of (PMMA-*g*-PSt-*g*-PU)/ZnAl LDH nanocomposite. The chemical properties of all prepared materials were studied by ^{1}H NMR and Fourier Transform Infrared spectroscopy (FTIR). The morphologies of the neat PU, PU-*g*-PSt, and a (PMMA-*g*-PSt-*g*-PU)/ZnAl LDH nanocomposite were examined by SEM and TEM. The thermal properties of the PU-*g*-PSt, (PMMA-*g*-PSt-*g*-PU) terpolymer and its LDH nanocomposite were studied by DSC and TGA analysis.

2. Experimental

2.1. Materials

The neat PU was prepared by the method previously obtained from our research group in laboratory [42,43]. (2,2′-bipyridine), CuBr, and all other chemicals were acquired from Merck and used without purification. DMF (*N*,*N*-dimethylformamide) was dried on CaH_2 and distilled before use. St (styrene) and MMA (Methyl Methacrylate) (both with a purity of 99%) were acquired from Sigma-Aldrich and redistilled with CaH_2 to remove the inhibitor prior to use. AIBN (2, 2′-azobisisobutyronitrile) was acquired from Aldrich and recrystallized in ethanol at 50°C. 9-decen-1-ol was acquired from Merck and used as received. Al $(NO_3)_3.9H_2O$ (aluminum nitrate) (99.4%, Hamburg Chemicals Co.), Zn $(NO_3)_2.6H_2O$ (98%, system) (zinc nitrate), Sodium Dodecyl Sulfate (SDS), NaOH (Merck Co., 99%) were obtained by Aldrich-Sigma and used as received.

2.2. Characterization and analyses

FTIR spectrum was recorded using Shimadzu FTIR-8101M (Japan, Kyoto, Shimadzu) at room temperature within the wave numbers range of 400 to 4000 cm^{-1}, with an attenuated whole reflection instrument. In order to the preparation of samples, the dry powders were grounded with KBr (potassium bromide) powder and compressed the admixture into disks. The disks were reserved in a desiccator to remove humidity absorption. XRD spectrum were provided with a Siemens D 5000 (USA, Texas, and Aubrey). X-ray generator (Cu K_α radiation with $\lambda = 1.5607$Å) with a 2θ scan range of 2 to 60° at room temperature. The proton nuclear magnetic resonance (^{1}HNMR) spectroscopy was carried out at 30°C using a 400 MHz (FT-NMR) Brucker spectrometer (Germany, Ettlingen, Brucker). The synthesized materials for ^{1}H NMR spectroscopy was provided by dissolving about 12 mg of products in 8 ml of DMF as solvent. The determine morphologies and size distribution of the prepared nanoparticles were performed using a SEM (type 1430 VP (UK, Cambridge, LEO Electron Microscopy) and TEM (The Netherlands, Eindhoven, Philips, CM10-TH microscope) with a 100 KV accelerator voltage. The thermal particularity of the prepared nanoparticles was studied by TGA-PL STA 1640 apparatus (UK, Shropshire, and Polymer Laboratories). The TGA experiments were conducted for about 10 mg of the sample under flowing atmosphere from 600°C to room temperature with heating and cooling rate of 10°Cmin^{-1}. The results of DSC analysis were carried out with a Netzsch (Germany, Selb)-DSC 200 F_3 Maia. The synthesized material was first heated to 250°C and then allowed to cool for 5 minutes to remove the thermal history. Following that, the material was reheated to 250°C at a rate of 10°Cmin^{-1}. The entire test was employed at a flow rate of 50 mLmin^{-1} under flowing purge.

2.3. Preparation of Zn-Al-LDH

The preparation of Zn-Al-LDH precursors at different pH values with a fixed molar ratio of Zn/Al=2 has been accomplished using the precipitation method. The synthesis was performed by a slow increase of two metal nitrates solutions which were Zn $(NO_3)_3.9H_2O$ (0.3 M) and Al $(NO_3)_3.6H_2O$ (0.08 M) with fixed stirring. The pH value for all synthesized samples was controlled by a drop-wise increase of NaOH solution (0.5 M). Titration of NaOH was employed under a N_2 purification to minimize or remove the contamination of produced CO_2 from the reaction medium. The resulting slurry was aged at 80°C for 20 hr in an oil bath shaker (70 rpm). The precipitate was washed several times with deionized water and dried for two days at room temperature in a vacuum oven.

2.4. Preparation of surfactant-modified Zn-Al (SDS)

The surfactant-modified Zn-Al-LDH was prepared through an anion exchange reaction of 2.0 g ZnAl (NO_3) with 100 mL 0.2 M SDS at 60°C. For this purpose, 2.0 g Zn-Al-LDH was dispersed into 150 mL decarbonated water by ultrasonic vibration for about 20 minutes. Next, 100 mL (0.2 M) SDS was slowly poured into suspension, then the produced slurry with a magnetic pellet was stirred intensely for 24 hr at 60°C temperature. Following that, the mixture reaction was precipitated in ice methanol and washed several times with distilled water and dried in a vacuum oven at 60°C.

2.5. Synthesis of PU macromolecular monomer

0.071 g (0.54 mmol) sample of neat PU, 50 mL of dry DMF, and 9-decen-1-ol were dissolved in a 250 mL three-necked flask fitted with a gas inlet/outlet, a condenser and a magnetic stirring bar. After refluxing at 80°C for 4 hr, the solution was filtered, half of the solvent was vaporized, and the PU macromolecular was precipitated in ice methanol. After dissolving in methanol, the solution was kept overnight to recrystallize the obtained product. After that, the solution was precipitated in ice methanol and the resultant macroinitiator was filtered, then washed with cold ether and dried in a vacuum.

2.6. Synthesis of PU-g-PSt

PU-*g*-PSt was successfully synthesized through free radical copolymerization of PU-macromolecular with styrene as a monomer, AIBN (2,2′-azobisisobutyronitrile) as initiator, and anhydrous DMF (*N*,*N*-dimethylformamide) as solvent. PU-macromolecular momomer, styrene, DMF and AIBN were added successively into a reaction mixture. After 1.5 hr of polymerization at 70°C, the reaction was done. Following that, the solution was precipitated in ice methanol and the resulting polymerization was dried under vacuum.

2.7. Synthesis of (PMMA-g-PSt-g-PU)/ZnAl LDH nanocomposite

2.7.1. Synthesis of (PU-g-PSt)–Br

In a 150 three-necked glass flask equipped with a dropping funnel and a reflux condenser, the bromination reactions were successfully performed. Thirty-three millimole of NBS and AIBN (0.05 g) was dissolved in 30 mL dried CCl_4 and were added under nitrogen flowing to a stirred solution CCl_4 (40 mL) of PU-*co*-PSt (0.5 g). The reaction mixture was stirred for 3 hr at 80 temperatures and poured into 300 mL of ice methanol to afford precipitate. The resulting product, after dissolving in THF was precipitated in cold methanol. The obtained precipitate was filtered and dried under a vacuum at room temperature. Product: 1.16 gr (white powder) (see Schemes 1 and 2).

2.7.2. Synthesis of (PMMA-g-PSt-g-PU) terpolymer via ATRP technique

In a common method, a 150 mL round-bottomed glass flask equipped with a magnetic stirring bar was charged with CCl_4 (15 mL), CuBr (0.06 g, 0.47 mmol), 2, 2-bipyridinyl (0.14 g, 0.95 mmol), MMA (2 mL, 21 mmol), and brominated (PU-*g*-PSt) (0.2 g). After stirring the contents of the flask with a magnetic stirrer, the flask was sealed and to eliminate oxygen, three cycles of a freeze-pump thaw were excreted. Following that, the flask was filled with purged N_2 and the reaction mixture was heated while stirring at 90°C for 10 hr. At the end of this time, the reaction was successfully completed by pouring the contents of the flask into ice methanol. The precipitated polymer was filtered, washed, and dried under a vacuum oven. The powder produced was extracted with cyclohexane at 30°C three times to eliminate PMMA it was formed as a homopolymer (see Scheme 2).

2.7.3. Preparation of (PMMA-g-PSt-g-PU)/ZnAl LDH nanocomposite

The (PMMA-*g*-PSt-*g*-PU)/ZnAl LDH nanocomposite was successfully prepared through the solution intercalation method. First, a desirable amount (0.05 g) of Zn-Al-(SDS) was refluxed in 100 mL DMF for 24 hr under nitrogen flow. Afterward, 1.0 g PMMA-*g*-

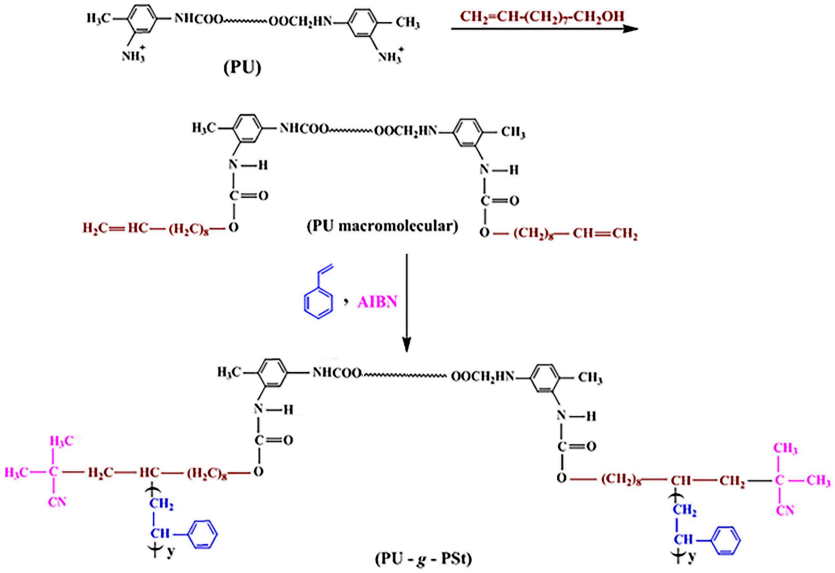

Scheme 1. Synthesis of (PU-*g*-PSt) graft copolymer.

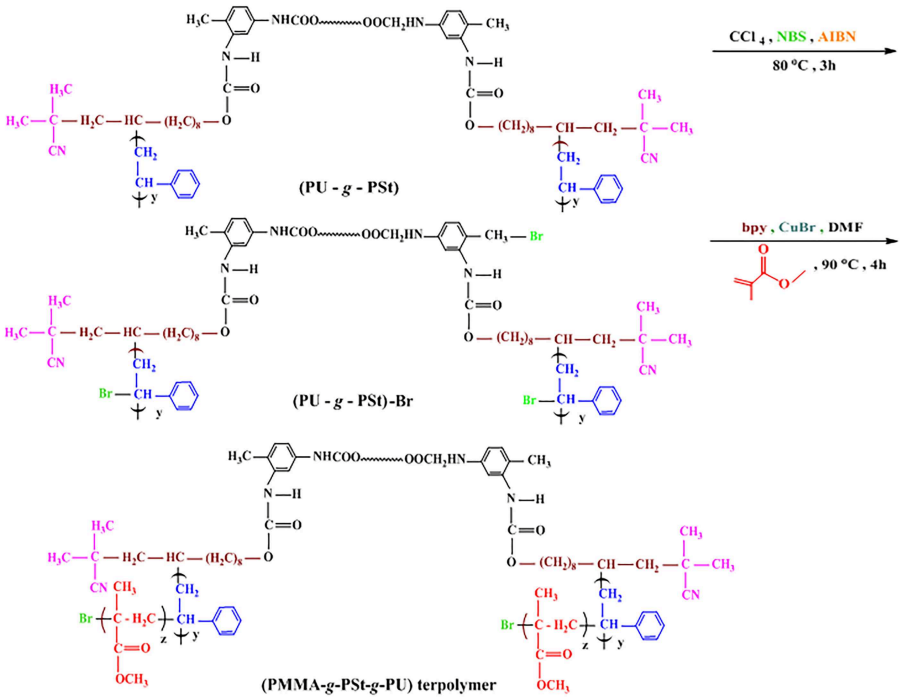

Scheme 2. The overall strategy for synthesis of (PMMA-*g*-PSt-*g*-PU) terpolymer

PSt-*g*-PU terpolymer was added into the Zn-Al-(SDS) suspension. After stirring for about 3 hr at 80°C, the contents of the flask were poured into ice methanol to precipitate. The resulting precipitate was filtered and dried under vacuum at room temperature for 2 days (see Scheme 3).

3. Result and discussion

3.1. Characterization of the PU-g-PSt graft copolymer and (PMMA-g-PSt-g-PU) terpolymer

The FTIR spectrum of PU-*g*-PSt, (PU-*g*-PSt)-Br and (PMMA-*g*-PSt-g) terpolymer are shown in Figure 1. The FTIR spectrum of the PU-*g*-PSt displayed some characteristics absorption bands including, the stretching vibration of -C-H aliphatic and aromatic appeared at (3100–2900 cm^{-1}), γ (C-H) in the aromatic ring appeared at 652 cm^{-1} and 785 cm^{-1}, the bending vibrations of -CH_2 group appeared at 1321 and 1425 cm^{-1}, the stretching vibrations of C=C observed at 1650 cm^{-1}, the stretching vibration of C=O groups observed at 1780 cm^{-1}, and the stretching vibrations of the -NH group observed at 3620 cm^{-1} [44].

The FTIR spectrum of (PU-*g*-PSt)-Br displayed an additional absorption peak at 557 cm^{-1} that related to the C-Br group. The FTIR spectra of (PMMA-*g*-PSt-*g*-PU) terpolymer exhibited the usual bands attributed to the PU chain, PMMA, and PSt segments. In this simple, the most significant absorption bands could be as follows: the stretching vibrations of the

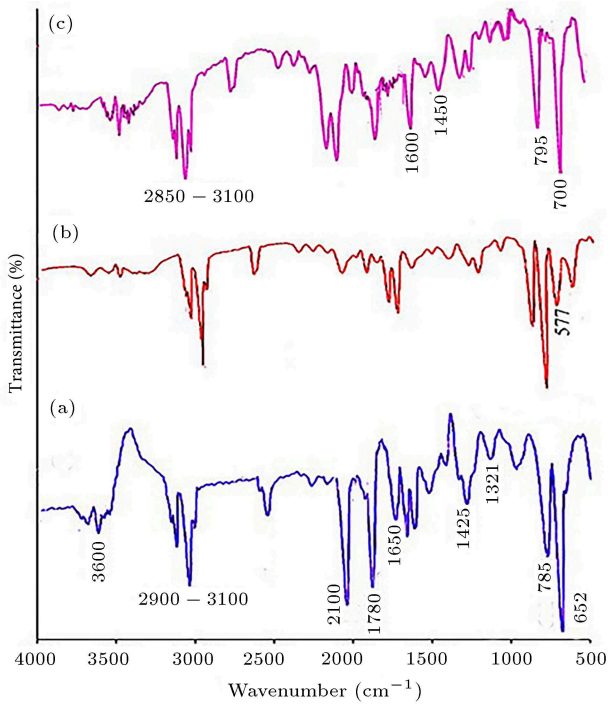

Figure 1. The FTIR spectra of (PU-*g*-PSt) (a), (PU-*g*-PSt)-Br (b) and (PMMA-*g*-PSt-*g*-PU)/LDH nanocomposite (c).

-C-H aliphatic and aromatic at 3100 to 2850 cm^{-1}, the stretching vibration of C–O at 1480 cm^{-1}, the stretching vibration of aromatic C=C at 1600 cm^{-1}, the stretching vibration of γ (C–H) in the aromatic ring at 700 cm^{-1} and 795 cm^{-1}.

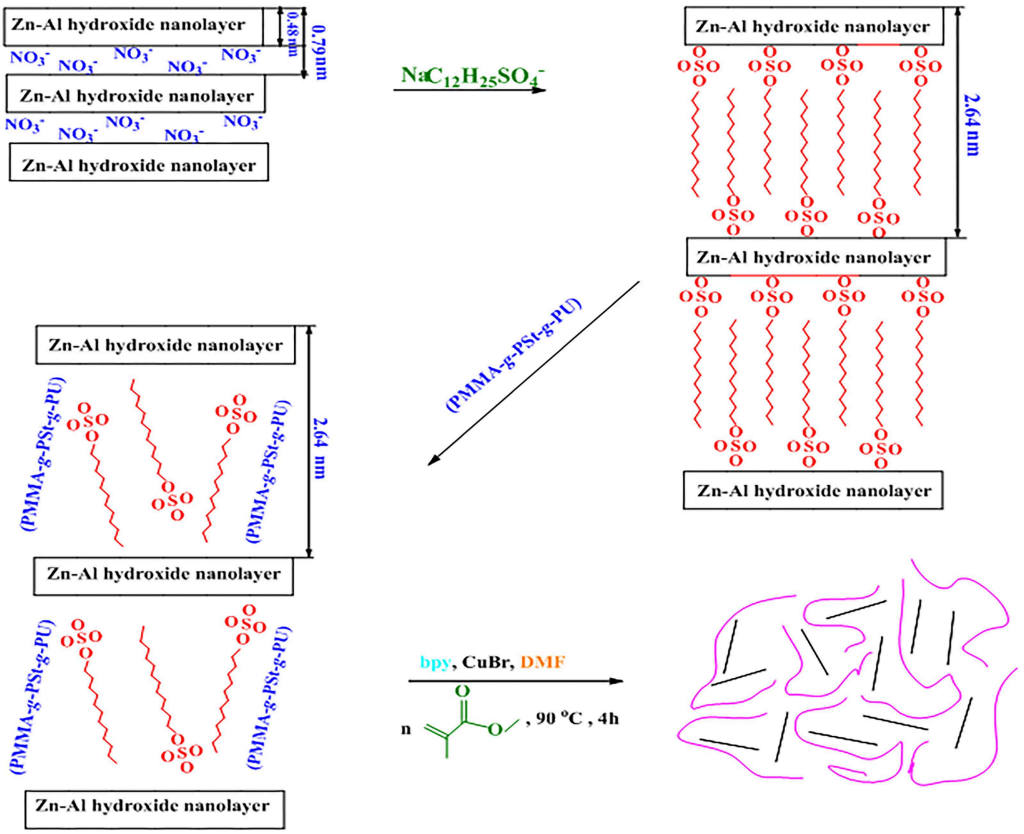

Scheme 3. Synthesis of (PMMA-*g*-PSt-*g*-PU)/Zn-Al-LDH nanocomposite.

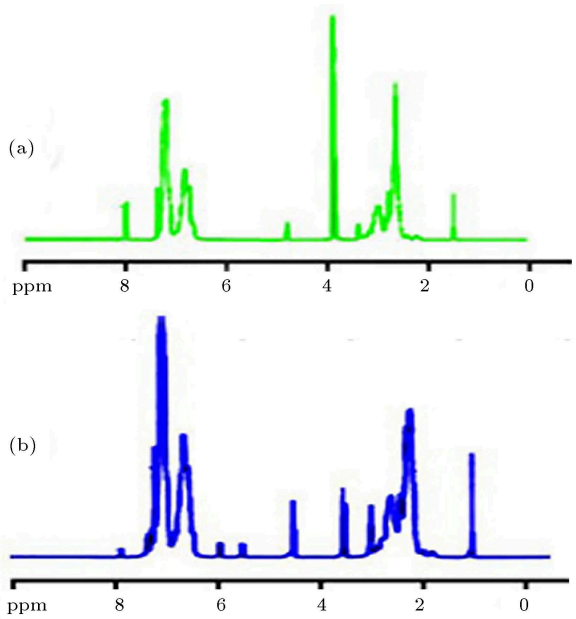

Figure 2. ^{1}H-NMR spectra of PU-*g*-PSt (a) and (PMMA-*g*-PSt-*g*-PU) (b).

Figure 2, displays the ^{1}H NMR spectrum of PU-*g*-PSt (a) and (PMMA-*g*-PSt-*g*-PU) terpolymer (b) recorded in DMF. The ^{1}H-NMR spectra of PSt-*g*-PU graft copolymer and (PMMA-*g*-PSt-*g*-PU) terpolymer displayed the resonance at about 1.86, 2.2 – 3.0, and 3.45 ppm, which attributed to the CH_3, CH_2, and CH in copolymer and terpolymer. Also, the resonances at around 6.15–7.41 ppm are attributed to aromatic protons and resonance at about 8.0 ppm attributed to the NH_2 group in urethane graft copolymer and terpolymer.

3.2. X-ray diffraction study

In the synthesis of a nanocomposite, X-Ray Diffraction (XRD) is employed to represent evidence on the changing interlayer interval of the LDH and study of polymer/clay nanocomposite. The making of an intercalated structure should lead to a decrease in 2θ, stating an increase in the d-interval in the making of a foliated structure. The XRD samples of surfactant-modified Zn-Al (SDS), Zn-Al-LDH and (PMMA-*g*-PSt-*g*-PU)/Zn-Al-LDH nanocomposite is seen in Figure 3. The XRD sample of Zn-Al-LDH, Figure 3(a) can be well indexed in a hexagonal lattice with an R-3m rhombohedral symmetry that is generally employed for the statement of the LDH nanoparticle structure. Purged cell parameters are a=3.064 A°(=2 × d_{110}) and c=26.217 A°(=3 × d_{003}). The most important spacing of the Zn-Al-LDH sample is 8.9 nm. The average crystallite size (D) of the synthesized Zn-Al-LDH was calculated by means Sherrer-Debye formula

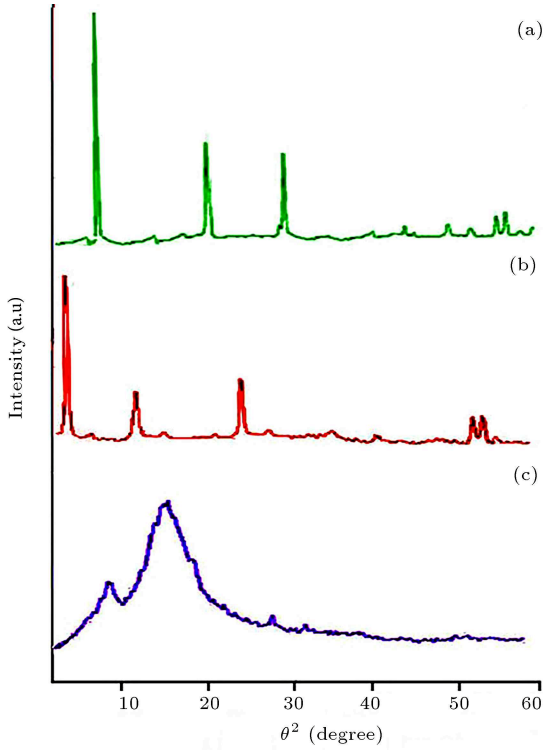

Figure 3. XRD patterns of Zn-Al-LDH (a) Zn-Al (SDS) (b) and (PU-*g*-PSt-*g*-PMMA)/Zn-Al-LDH nanocomposite (c).

D = Kk/$\beta\cos\theta$) [45,46], which was nearly at around 37.51 nm. In Figure 3(b), the most important spacing of Zn-Al (SDS) sample increases 1.20 to 11.2 nm ($2\theta = 11$ to $2\theta = 3$) of Zn-Al-LDH sample after the (NO_3^-) ion in this sample exchanged through SDS, which displays the SDS anions in the Zn-Al-LDH layers have been successfully intercalated. Figure 3(c), shows the XRD samples of (PMMA-*g*-PSt-*g*-PU)/LDH nanocomposite in the range of 2β=10°–60°. It is shown visibly that Zn-Al-LDH layers in the PU-*g*-PSt/LDH nanocomposite and (PU-*g*-PSt-*g*-PMMA)/LDH nanocomposite matrix have been much exfoliated. Furthermore, the peak at $2 - \theta = 18$ attributed to pristine PSt and PMMA.

3.3. Characterization (PMMA-g-PSt-g-PU)/LDH nanocomposite

The thermal behaviors of neat PU and (PMMA-*g*-PSt-*g*-PU)/ZnAl LDH nanocomposite were studied by TGA and DSC as seen in Figures 4 and 5. As shown, the thermal decomposition of neat PU occurs in the weight loss at the range of 110–390°C and no residuals are left upper 390°C. The results of TGA display modification of the thermal stability for (PMMA-*g*-PSt-*g*-PU)/LDH nanocomposite (4 w.t% LDH) in comparison with neat PU. The thermal decomposition with the maximum rate of weight loss for neat PU and (PU-*g*-PSt-*g*-PMMA)/LDH nanocomposite is 180.5°C,

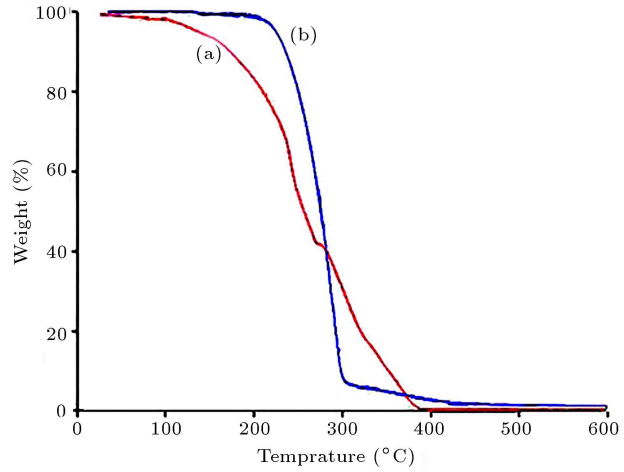

Figure 4. TGA trace of neat PU (a) and (PMMA-*g*-PSt-*g*-PU)/Zn-Al-LDH nanocomposite (b).

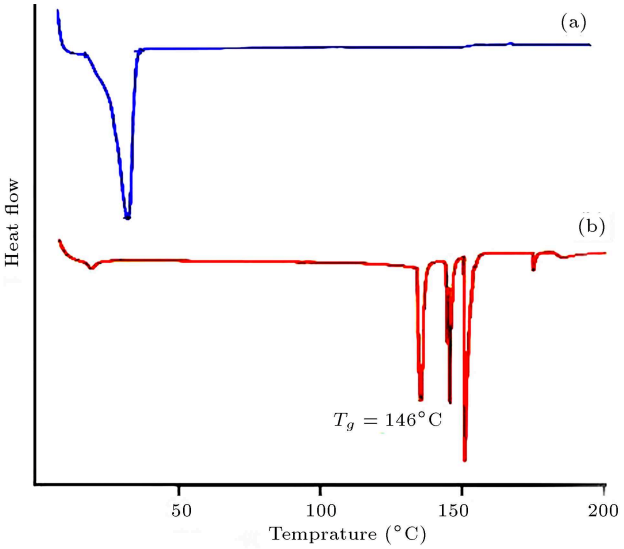

Figure 5. DSC trace of pure PU (a) and (PMMA-*g*-PSt-*g*-PU)/Zn-Al- LDH nanocomposite (b)

and 255.6°C, respectively [47]. These results exhibit that the thermal stability of the exfoliated material improves significantly. The increase in thermal stability for the nanocomposite may be attributed to a decline in oxygen and temporary degradation products penetrability/diffusion that derived from the hindrance influence of the exfoliated LDH layers in the PSt and PMMA matrix.

On the other hand, The DSC trace of neat PU and (PMMA-*g*-PSt-*g*-PU)/ZnAl LDH nanocomposite are shown in Figure 5. The neat PU in Figure 5(a) displays an enthalpy peak at about 40°C that attributed to the T_g (glass transition temperature). Figure 5(b) displays an endothermic peak at 175°C attributed to the nanocomposite degradation. The transmission observed at 146°C can be assigned to the glass transmission of this nanocomposite [48]. PSt

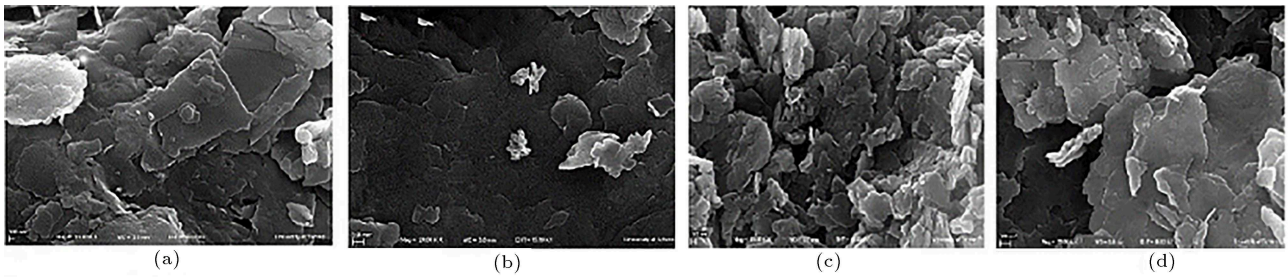

Figure 6. SEM images of Zn-Al-LDH (a,b) and Zn-Al (SDS) (c,d) at different magnifications.

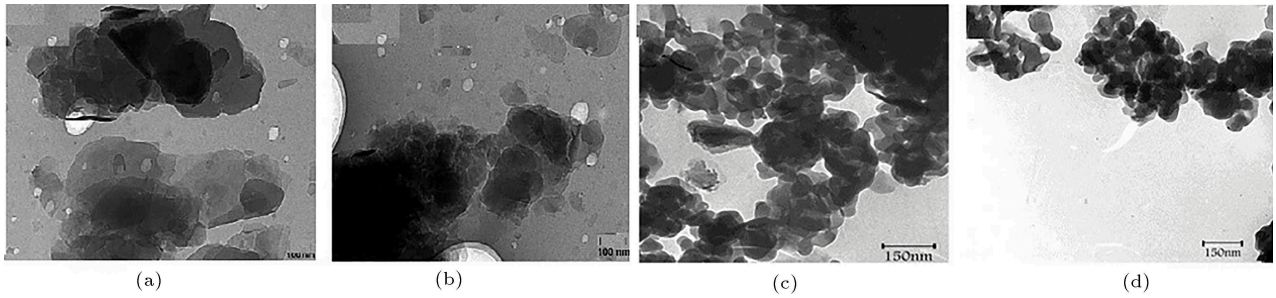

Figure 7. TEM images of the Zn-Al-LDH (a,b) and (PMMA-*g*-PSt-*g*-PU)/Zn-Al-LDH nanocomposite (c,d).

and PMMA chains bonded to the backbone of neat PU resulted in more flexibility in copolymer structure. As a result, it can be led to degradation at lower temperatures. The DSC thermogram also proves the deficiency of any melting for full of materials.

3.4. Morphology study

The morphologies behavior of the synthesized Zn-Al-LDH, Zn-Al (SDS), and (PMMA-*g*-PSt-*g*-PU)/Zn-Al-LDH nanocomposite was observed using SEM and TEM. The SEM image of Zn-Al-LDH indicates that the synthesized nanoparticles are sheet-like and their hexagonal structures are clear in Figure 6(a) and (b). The surface morphologies of Zn-Al (SDS) exhibited homogeneously distributed particles giving a relatively large surface of Zn-Al (SDS). This is much significant for synthesizing polymeric nanocomposite. Also, the dispersion is better and sheet-like; the surface nanoparticles approximately is clear in Figure 6(c) and (d).

On the other hand, it is accepted that TEM represents a factual image from the morphology of the synthesized LDH nanocomposite. The structure of the Zn-Al-LDH platelets was studied using TEM to evaluate the structural characterization of the polymer-LDH system and morphological behavior. Figure 7 displays the TEM of the oxide products provided on hydrothermal behavior of the LDH nanoparticle. The Zn-Al-LDH, on the hydrothermal decomposition at 150°C products a lot of matched crystallites of the spinel phase. In some areas, hexagonal prisms attributed to the ZnO (wurtzite) phase also could be observed. Nevertheless, the products gained on thermal decomposition of Zn-Al-LDH (400°C) which is related to neat ZnO do not reveal any specific morphological characteristic that are reflected without crystal growth under these conditions are shown in Figure 7(a) and (b). On the other hands, in the TEM micrograph of the (PMMA-*g*-PSt-*g*-PU)/Zn-Al-LDH nanocomposite as shown in Figure 7(c) and (d), is clear that the nanocomposites were in extremely exfoliated condition. In addition, the black lines demonstrate the LDH nanoparticles with a density of about 1 nm, and the inconspicuous lines indicate the polymer matrix. It is apparent from the investigation of TEM images that the LDH nanoparticles layers are interspersed slightly in a disordered mode in the polymer matrix. Furthermore, nano-sized LDH densities could be discovered in differing ratings, which relate to intercalated or nearly exfoliated structure of the nanocomposite. This examination with the results obtained from XRD could be resistant. If the LDH nanoparticles are interspersed homogeneously, and randomly in the polymer matrix, the interface region is large and pronounced interaction can be predicted.

Figure 8(a) and (b) indicates the percent frequency of Zn-Al-LDH nanoparticles and (PMMA-*g*-PSt-*g*-PU)/LDH nanocomposite, respectively. The graph shows the percentage of Zn-Al-LDH nanoparticles in the polymer. As can be seen, 48% dispersion of nanoparticles with a size of $20-30$ nm is seen in 6% of the polymer. And 36% dispersion of nanoparticles with a size of $30-40$ nm is seen in 22% of the polymer.

4. Conclusion

A novel method for preparing (PMMA-*g*-PSt-*g*-

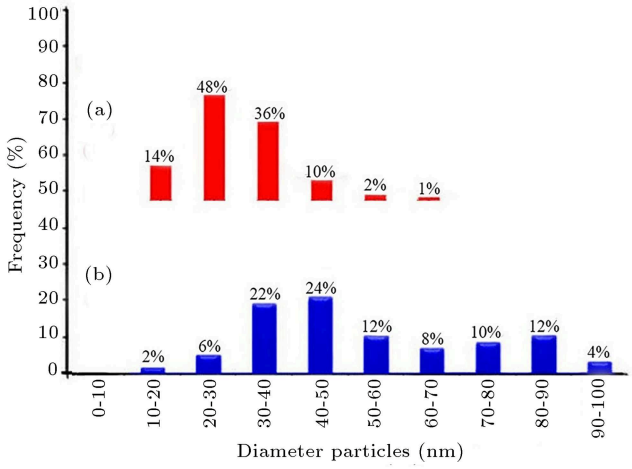

Figure 8. The curve present frequency of Zn-Al-LDH nanoparticle (a) and (PMMA-*g*-PSt-*g*-PU)/LDH nanocomposite (b).

PU)/Zn-Al-LDH nanocomposite through the combination of conventional and developed methods has been successfully demonstrated. The successful synthesis of PU-*co*-PSt copolymer and (PMMA-*g*-PSt-*g*-PU) terpolymer were proved using ^{1}H NMR and Fourier Transform Infrared Spectroscopy (FTIR). FE-SEM images verified that surface morphologies of Zn-Al (SDS) and Zn-Al-LDH led to the sheet-like and hexagonal morphology. Investigation of thermal properties using DSC and TGA exhibited that the prepared (PMMA-*g*-PSt-*g*-PU)/Zn-Al-LDH nanocomposite has higher properties compared to neat PU. The most important cause for higher properties of the (PMMA-*g*-PSt-*g*-PU)/Zn-Al-LDH nanocomposite may be derived from intense interaction between polymer matrix and LDH layers. TEM observation revealed that produced nanocomposite was in the completely exfoliated condition and LDH nanoparticles with about 1 nm thickness were dispersed partly in a disordered mode in the nanocomposite, which led to the strong interaction between polymer matrix and LDH modified with Sodium Dodecyl Sulfate (SDS). The synthesized terpolymer and (PSt-*g*-PU-*g*-PMMA)/LDH nanocomposite can be used as a reinforcing agent for polymeric nanocomposites material due to the high properties of LDH.

Acknowledgments

The authors express their sincere thanks to Payame Noor University for the financial support of this work.

Conflict of interest

The authors declare no conflict of interest.

References

1. Park, J.S., Lim, Y.M., and Nho, Y.C. "Preparation of high-density polyethylene/waste polyurethane blends compatibilized with polyethylene-graft-maleic anhydride by radiation", *Materials*, **8**(4), pp. 1626–1635 (2015). DOI: 10.3390/ma8041626
2. Park, J.S., Lim, Y.M., and Nho, Y.C. "Radiation-induced grafting with one-step process of waste polyurethane onto high-density polyethylene", *Materials*, **9**(1), p. 13 (2016). DOI: 10.3390/ma9010013
3. Simon, D., Garcia, M.T., Lucas, A.D., et al. "Glycolysis of flexible polyurethane wastes using stannous octoate as the catalyst: Study on the influence of reaction parameters", *Polymer Degradation and Stability*, **98**(1), pp. 144–149 (2013). DOI: 10.1016/j.polymdegradstab.2012.10.017
4. Beyer, G. "Flame retardant properties of EVA-nanocomposites and improvements by combination of nanofillers with aluminium trihydrate", *Fire and Materials*, **25**(5), pp. 193–197 (2001). DOI: 10.1002/fam.776
5. Kim, J.H. and Kim, S.C. "Controlling the morphology of polyurethane/polystyrene interpenetrating polymer networks for enhanced blood compatibility", *Journal of Applied Polymer Science*, **84**(2), pp. 379–387 (2002). DOI: 10.1002/app.10358
6. Tanobe, V.O.A., Sydenstricker, T.H.D., Amico, S.C., et al. "Evaluation of flexible postconsumed polyurethane foams modified by polystyrene grafting as sorbent material for oil spills", *Journal of Applied Polymer Science*, **111**(4), pp. 1842–1849 (2009). DOI: 10.1002/app.29180
7. Duong, H.T.T. and Burford, R.P. "Effect of foam density, oil viscosity, and temperature on oil sorption behavior of polyurethane", *Journal of Applied Polymer Science*, **99**(1), pp. 360–367 (2006). DOI: 10.1002/app.22426
8. Koenig, A., Ziener, U., Schaz, A., et al. "Polyurethane-block-polystyrene prepared by polymerization in miniemulsion", *Macromolecular Chemistry and Physics*, **208**(2), pp. 155–163 (2007). DOI: 10.1002/macp.200600448
9. Calvete, D.P., Holguin, D.F.R., and Luna, M.P. "Development of styrene-grafted polyurethane by radiation-based techniques", *Procedia Material Science*, **9**(6), p. 491 (2015).
10. Jahny, K., Adler, H.P., and Moritz, H. "Kinetics of aqueous heterophase polymerization of styrene with polyurethane emulsifier", *Macromolecular Chemistry and Physics*, **202**(14), pp. 2915–2920 (2001). DOI: 10.1002/1521-3935(20011001)202:143.0.CO;2-B
11. Gupta, B., Srivastava, A., Grover, N., et al. "Plasma induced graft polymerization of acrylic acid onto poly (ethylene terephthalate) monofilament", *Indian Journal of Fibre and Textile*, **35**(1), pp. 9–14 (2010).
12. Rong, M.Z., Ji, Q.L., Zhang, M.Q., et al. "Graft polymerization of vinyl monomers onto nano-sized alumina particles", *European Polymer Journal*, **38**(8), pp. 1573–1582 (2002). DOI: 10.1016/S0014-3057(02)00037-X

13. Chan, C.M. and KO, T.M. "Polymer surface modification by plasmas and photons", *Surface Science Reports*, **24**(1–2), pp. 1–54 (1996). DOI: 10.1016/0167-5729(96)80003-3

14. Abbasian, M., Masoumi, B., and Rashidzadeh, B. "Versatile method via reversible addition-fragmentation transfer polymerization for synthesis of poly styrene/ZnO–nanocomposite", *Polymer Engineering and Science*, **56**(2), pp. 187–195 (2016). DOI: 10.1002/pen.24242

15. Hatamzadeh, M. and Jaymand, M. "Synthesis of conductive polyaniline-modified polymers via a combination of nitroxide-mediated polymerization and "click chemistry", *RSC Advances*, **54**(4), pp. 28653–28663 (2014). DOI: 10.1039/c4ra00864b

16. Wang, J.S. and Matyjaszewski, K. "Controlled/living" radical polymerization. Atom transfer radical polymerization in the presence of transition-metal complexes", *Journal of the American Chemical Society*, **117**(20), pp. 5614–5615 (1995). DOI: 10.1021/ja00125a035

17. Abbasian, M., Jaymand, M., and Esmaeily Shoja, S. "Synthesis and characterization of a terpolymer derived from styrene, methyl styrene, and polyaniline and its organoclay nanocomposite", *Journal of Applied Polymer Science*, **125**(21), pp. 131–140 (2012). DOI: 10.1002/app.35391

18. Jaymand, M., Hatamzadeh, M., and Omidi, Y. "Modification of polythiophene by the incorporation of processable polymeric chains: Recent progress in synthesis and applications", *Progress in Polymer Science*, **47**, pp. 26–69 (2015). DOI: 10.1016/j.progpolymsci.2014.11.004

19. Abbasian, M., Bakhshi, M., Jaymand, M., et al. "Nitroxide-mediated graft copolymerization of styrene from cellulose and its polymer/montmorillonite nanocomposite", *Journal of Elastomers and Plastic*, **51**(5), pp. 1–17 (2018). DOI: 10.1177/00952443187994

20. Karaj-Abad, S.G., Abbasian, M., and Jaymand, M. "Grafting of poly [(methyl methacrylate)-block-styrene] onto cellulose via nitroxide-mediated polymerization, and its polymer/clay nanocomposite", *Carbohydrate Polymers*, **152**(5), pp. 297–305 (2016). DOI: 10.1016/j.carbpol.2016.07.017

21. Nicolas, J., Guillaneuf, Y., Lefay, C., et al. "Degradable and comb-like PEG-Based copolymers by nitroxide-mediated radical ring-opening polymerization", *Progress in Polymer Science*, **14**(10), pp. 3769–3779 (2013). DOI: 10.1021/bm401157g

22. Mohammad-Rezaei, R., Massoumi, B., Eskandani, M., et al. "A new strategy for the synthesis of modified novolac resin and its polymer/clay nanocomposite", *Express Polymer Letters*, **13**(6), pp. 543–552 (2019). DOI: 10.3144/expresspolymlett.2019.46

23. Rafiei, H., Abbasian, M., and Yegani, R. "Synthesis of well-defined poly (n-vinylpyrrolidone)/n-TiO_2 nanocomposites by xanthate-mediated radical polymerization", *Iranian Polymer Journal*, **29**(5), pp. 371–381 (2020). DOI: 10.1007/s13726-020-00795-8

24. Abbasian, M., Hasanzadeh, P., Mahmoodzadeh, F., et al. "Novel cationic cellulose-based nanocomposites for targeted delivery of methotrexate to breast cancer cells", *Macromolecular*, **57**(2), pp. 99–115 (2020). DOI: 10.1080/10601325.2019.1673174

25. Abbasian, M., Razavi, L., Jaymand, M., et al. "Synthesis and characterization of poly (styrene-block-acrylic acid)/Fe_3O_4 magnetic nanocomposite using reversible addition-fragmentation chain transfer polymerization", *Scientica Iranica*, **26**(3), pp. 1447–1456 (2019). DOI: 10.24200/sci.2019.21232

26. Mahmoodzadeha, F., Abbasian, M., Jaymandc, M., et al. "A novel gold-based stimuli-responsive theranostic nanomedicine for chemo-photothermal therapy of solid tumors", *Materials Science and Engineering*, **93**, pp. 880–889 (2018). DOI: 10.1016/j.msec.2018.08.067

27. Abbasian, M., Seyyedi, M., and Jaymand, M. "Modification of thermoplastic polyurethane through the grafting of well-defined polystyrene and preparation of its polymer/clay nanocomposite", *Polymer Bulletin*, **77**(3), 1107–1120 (2020). DOI: 10.1007/s00289-019-02773-4

28. Abbasian, M., Ghaeminia, H., and Jaymand, M. "A facile and efficient strategy for the functionalization of multiple-walled carbon nanotubes using well-defined polypropylene-grafted polystyrene", *Applied Physics A.*, **124**(522), pp. 1–9 (2018). DOI: 10.1007/s00339-018-1943-4

29. Rafiei, H., Abbasian, M., and Yegani, R. "Synthesis of well-defined poly (n-vinylpyrrolidone)/n-TiO_2 nanocomposites by xanthate-mediated radical polymerization", *Iranian Polymer Journal*, **29**, pp. 371–381 (2020). DOI: 10.1007/s13726-020-00795-8

30. Massoumi, B., Abbasian, M., Mohammad, R.R., et al. "Polystyrene-modified novolac epoxy resin/clay nanocomposite: Synthesis, and characterization", *Polymers Advanced Technologies*, **30**(6), pp. 1484–1492 (2019). DOI: 10.1002/pat.4580

31. Matyjaszewski, K. and Tsarevsky, N.V. "Macromolecular engineering by atom transfer radical polymerization", *Journal of the American Chemical Society*, **136**(18), pp. 6513–6533 (2014). DOI: 10.1021/ja408069v DOI: 10.1039/c4py01457j

32. Xue, Z., He, D., and Xie, X. "Iron-catalyzed atom transfers radical polymerization", *Polymer Chemistry*, **6**(10), pp. 1660–1687 (2015).

33. Summerlin, B.S., Tsarevsky, N.V., Louche, G., et al. "Highly efficient "click" functionalization of poly (3-azidopropylmethacrylate) prepared by ATRP", *Macromolecules*, **38**, pp. 7540–7545 (2005). DOI: 10.1021/ma0511245

34. Chiu, C.W., Huang, T.K., Wang, Y.C., et al. "Intercalation strategies in clay/polymer hybrids", *Progress in Polymer Science*, **39**(3), pp. 443–485 (2014). DOI: 10.1016/j.progpolymsci.2013.07.002

35. Abbasian, M., Pakzad, M., and Amirmanesh, M. "Polymericaly modified clays to preparation of

polystyrene nanocomposite by nitroxide mediated radical polymerization and solution blending methods", *Polymer Composites*, **38**(6), pp. 1127–1134 (2017). DOI: 10.1002/pc.23675

36. Sarbu, T., Lin, K.Y., Spanswick, J., et al. "Synthesis of hydroxy-telechelic poly (methyl acrylate) and polystyrene by atom transfer radical coupling", *Macromolecules*, **37**(26), pp. 9694–9700 (2004). DOI: 10.1021/ma0484375

37. Zare, Y. and Garmabi, H. "Thickness, modulus and strength of interphase in clay/polymer nanocomposites", *Applied Clay Science*, **66**(105–106), pp. 66–70 (2015). DOI: 10.1016/j.clay.2014.12.016

38. Madusanka, N., De Silva, K.M.N., and Amaratunga, G. "A curcumin activated carboxymethyl cellulose-montmorillonite clay nanocomposite having enhanced curcumin release in aqueous media", *Carbohydrate Polymers*, **134**, pp. 695–699 (2015). DOI: 10.1016/j.carbpol.2015.08.030

39. Kotal, M. and Bhowmick, A.K. "Polymer nanocomposites from modified clays: Recent advances and challenges", *Progress in Polymer Science*, **51**, pp. 127–187 (2015). DOI: 10.1016/j.progpolymsci.2015.10.001

40. Suter, J.L., Groen, D., and Coveney, P.V. "Chemically specific multiscale modeling of clay–polymer nanocomposites reveals intercalation dynamics, tactoid self-assembly and emergent materials properties", *Advanced Materials*, **27**, pp. 966–984 (2015). DOI: 10.1002/adma.201403361

41. Chu, C.C., Chiang, M.L., Tsai, C.M., et al. "Exfoliation of montmorillonite clay by mannich polyamines with multiple quaternary salts", *Macromolecules*, **38**(15), pp. 6240–6243 (2005). DOI: 10.1021/ma0503716

42. Moon, S.Y., Kim, J.K., and Lee, C.N. "Polyurethane/montmorillonite nanocomposites prepared from crystalline polyols, using 1, 4-butanediol and organoclay hybrid as chain extenders", *European Polymer Journal*, **40**(8), pp. 1615–1621 (2004). DOI: 10.1016/j.eurpolymj.2004.04.018

43. Pattanyak, A. and paul, D.R. "Morphology and properties of thermoplastic polyurethane nanocomposites: Effect of organoclay structure", *Polymer*, **47**(22), pp. 7760–7773 (2006). DOI: 10.1016/j.polymer.2006.08.067

44. Xu, Y., Petrovic, Z., Das, S., et al. "Morphology and properties of thermoplastic polyurethanes with dangling chains in ricinoleate-based soft segments", *Polymer*, **49**(19), pp. 4248–4258 (2008). DOI: 10.1016/j.polymer.2008.07.027

45. Uemura, T., Kaseda1, T., Sasaki, Y., et al. "Mixing of immiscible polymers using nanoporous coordination templates", *Nature Communications*, **6**, pp. 1–8 (2015). DOI: 10.1038/ncomms8473

46. Abbasian, M., Seyyedi, M., and Jaymand, M. "Modifcation of thermoplastic polyurethane through the grafting of well-defned polystyrene and preparation of its polymer/clay nanocomposite", **77**(3), pp. 1107–1120 (2019). DOI: 10.1007/s00289-019-02773-4

47. Mozaffari, Z., Hatamzadeh, M., Massoumi, B., et al. "Synthesis and characterization of a novel stimuli-responsive magnetite nanohydrogel based on poly (ethylene glycol) and poly(N-isopropylacrylamide) as drug carrier", *Journal of Applied Polymer Science*, **135**(36), pp. 46657–46657 (2018). DOI: 10.1002/app.46657

48. Farnoudian, A. H., Kangari, S., Massoumi, B., et al. "Determination of losartan potassium in the presence of hydrochlorothiazide via a combination of magnetic solid phase extraction and fluorometry techniques in urine samples", *RSC Advances*, **5**(124), pp. 102895–102903 (2015). DOI: 10.1039/c5ra20117a

Biographies

Mehdi Hosseinzadeh is Assistant Possessor at University of Tabriz, Tabriz, Iran. He received BSc degree in Applied Chemistry and MSc degree in Organic Chemistry (Polymer Science) from University of Tabriz in 2000 and 2002, respectively, and PhD degree in Organic Chemistry (Polymer Science) from Urmia University in 2015. His research interests include polymer chemistry, living radical polymerization, polymer adsorbents, nanocomposite polymers, and drug delivery system.

Saber Ghasemi Karaj-Abad received BSc degree in Pure Chemistry and MSc degree in Organic Chemistry (Polymer Science) from Payame Noor University, Tabriz, Iran, in 2014 and 2016, respectively. His research interests include living radical polymerization, nanocomposite polymers, and drug delivery system.

Mehdi Rasizadeh received BSc degree in Pure Chemistry and MSc degree in Organic Chemistry (Polymer Science) from Payame Noor University, Tabriz, Iran, in 2014 and 2016, respectively. His research interests include living radical polymerization, and nanocomposite polymers.

Mojtaba Abbasian is Professor in the Department of Chemistry at Payame Noor University, Tabriz, Iran. He received BSc degree in Pure Chemistry in 2000, and MSc and PhD degrees in Organic Chemistry (Polymer Science) in 2002 and 2007, respectively, all from University of Tabriz, Iran. His research interests include living radical polymerization, nanocomposite polymers, and drug delivery system.